Light Flash Studies

At the impact of a high-velocity projectile on a thick target a small fraction of the kinetic energy is converted to radiant energy. The light intensity as a function of time as well as the optical spectrum can be observed. Friichtenicht[8] used iron microparticles and observed the light flash by two-color photometry. He found that the blue part of the spectrum is increasing more rapidly with velocity than the red part. He observed a narrow (typically 0.2 μsec wide) fast risetime pulse of light followed by a much wider pulse (typically 10 μsec) which decays slowly to zero intensity. These observations are quite similar to results of Rollins and Jean[9] with bigger projectiles. They were able to measure more details because of the higher light intensity available. The projectiles were aluminum of cm size and were accelerated by a light gas gun. The target material was cadmium.

The first spike is continuum radiation and only present at the impact point. It is apparently due to a fast jet of material caused by the very high initial pressures. The peak intensity and the initial rate of change of intensity of the spike are proportional to v^8d^α and $v^6d^{2.1}$, respectively, with v = projectile velocity, d = projectile diameter, α = 2.9...4.0 (exact value depending on the wavelength used), and were found to be suitable to determine both diameter and velocity of a projectile if its composition is known.

The tail of the light flash is associated with a luminous ring expanding along the target plane. This ring is radiating in spectral lines which are characteristic of both target and projectile material. By analyzing the emission spectrum it is, in prinicpal, possible to determine the composition of the projectile.

Conclusion

As we have seen, there are three independent methods to determine velocity, mass, and composition of micrometeoroids. The light flash, however, is probably too faint and the emission spectrum too complicated as to lead to a practicable analysis. In order to investigate the crater, a very narrow beam of medium energy electrons and additional complicated instruments for electron and X-ray detection are necessary: volatile elements certainly escape observation. Analysis of the plasma seems to be the only practicable technique for micrometeoroid analysis onboard a spacecraft, although much additional effort is necessary to arrive at a quantitative method.

References

[1] Friichtenicht, J. F., Slattery, J. C., and Tagliaferri, E., "A Laboratory Measurement of Meteor Luminous Efficiency," *Astrophysical Journal*, Vol. 151, No. 1, Feb. 1968, pp. 747–758.

[2] Slattery, J. C. and Friichtenicht, J. F., "Ionization Probability of Iron Particles at Meteoric Velocities," *Astrophysical Journal*, Vol. 147, No. 1, Jan. 1967, pp. 235–244.

[3] Rudolph, V., "Untersuchungen an Kratern von Mikroprojektilen im Geschwindigkeitsbereich von 0,5 bis 10 km/sec," *Zeitschrift für Naturforschung*, Vol. 24a, No. 3, March 1969, pp. 326–331, English Translation NASA TT-F-11890.

[4] Neukum, G., "Untersuchungen des Projektilmaterials in Mikrokratern," Diplomarbeit, Universität Heidelberg, 1969, English Translation, NASA TT-F-12327.

[5] Grün, E. and Rauser, P., "Penetration Studies of Iron Dust Particles in Thin Foils," *Space Research*, Vol. IX, North-Holland Publishing Co., Amsterdam, 1969, p. 147.

[6] Auer, S. and Sitte, K., "Detection Technique for Micrometeoroids Using Impact Ionization," *Earth and Planetary Science Letters*, Vol. 4, No. 2, April 1968, pp. 178–183.

[7] Hansen, D. O., "Mass Analysis of Ions Produced by Hypervelocity Impact," *Applied Physics Letters*, Vol. 13, No. 3, Aug. 1968, pp. 89–91.

[8] Friichtenicht, J. F., "Experiments on the Impact-Light-Flash at High Velocities," NASA CR-416, March 1966, TRW Systems, Redondo Beach, Calif.

[9] Rollins, T. L. and Jean, B., "Impact Flash for Micrometeoroid Detection," NASA CR-92122, May 1968, Computing Devices of Canada, Ottawa, Ontario.

Determination of the Energy Balance of a Pulsed Plasma Source

R. Köhne* and A. Meert*

Deutsche Forschungs und Versuchsanstalt für Luft und Raumfahrt, E.V., Stuttgart, Germany

Introduction

Design of a continuously working inductive plasma accelerator requires knowledge of the efficiency of energy exchange into the plasma. For basic information, it is sufficient to study the process of ionization, acceleration and heating of a pulsed accelerator. It is possible to obtain an approximate determination of the energy balance on the complete system by spectroscopically determining particle temperature, plasma velocity, and the damping rate of the oscillatory circuit of the system.

Measuring Instrumentation

The pulsed inductive acceleration device has been described in detail in Refs. 1 and 2. Helium gas, passing through a quick acting electromagnetic valve, enters the acceleration tube (pyrex glass) which is evacuated to a pressure lower than 10^{-5} torr. The gas is ionized and accelerated by a single-turned conical coil across which a capacitor battery (6.5 μF, 10–15 kv) is discharged a defined time Δt (here 450 μs) after opening the valve.

Spectroscopic measurements are carried out with optical interference filters. Signals are led through fiber optics to photomultipliers where they are registered on an oscilloscope screen. The optical arrangement was attached on a support which could be shifted along the acceleration tube. Thus, the arrival of the plasmoids at different positions could be observed and velocities determined. Simultaneously, the damping of the oscillating current with and without plasma generation and acceleration was measured using a pick-up coil.

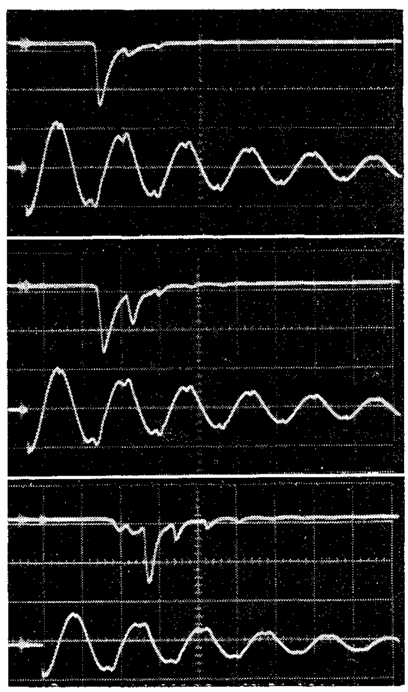

Fig. 1 Oscillograms of corresponding light intensities and pick-up voltages.

Received August 3, 1970; revision received October 13, 1970.

* Member of the Scientific Staff.

Results

In Fig. 1, typical oscillograms for three charging voltages (U = 15, 13.5, and 10 kv; from top to bottom) are presented. The upper signals show the corresponding light intensity of the He II (4686 Å) line emitted by the plasma. The lower signals are the pick-up coil voltages. The breakdown and simultaneous light emission for U = 15 kv take place after one oscillation period. With decreasing U, a second peak appears after 1.5 periods (second plasmoid) which finally overcomes the first peak, because the first peak continuously vanishes (for U = 10 kv).

The total power input E_{tot} distributes in

$$E_{tot} = CU^2/2 = E_0 + E_{pl} \quad (1)$$

where E_0 = losses in the circuit, E_{pl} = energy absorbed by the plasma, and E_{pl} distributes itself in

$$E_{pl} \simeq E_{ion} + E_{therm} + E_{kin} \quad (2)$$

where E_{ion} = ionization energy, E_{therm} = energy for plasma heating, and E_{kin} = kinetic energy of the accelerated plasma.

The value of E_{pl} can be determined in first approximation from the damping of the discharge current which is described in Ref. 3. A resistance $R_1 = R_0 + R_{pl}$ is introduced (R_0 = loss resistance, R_{pl} is an equivalent plasma resistance) which causes the same current as in the actual circuit. Thus, without plasma

$$E_{tot} = \int_0^\infty R_0 I_0^2(t)dt \quad (3a)$$

with plasma

$$E_{tot} = \int_0^\infty R_1 I_1^2(t)dt \quad (3b)$$

Defining the efficiency of energy transfer

$$\eta = E_{pl}/E_{tot} \quad (4)$$

where $I_0(t) = I_A f_0(t)$ and $I_1(t) = I_A f_1(t)$ then

$$\eta = 1 - \int_0^\infty f_0^2(t)dt \Big/ \int_0^\infty f_1^2(t)dt \quad (5)$$

The first amplitude I_A is equal for both currents (experimentally determined). With $f_0(t) = \exp(-\alpha_0 t)\sin\omega t$ and $f_1(t) = \exp(-\alpha_1 t)\sin\omega t$, the efficiency simplifies under the condition $\omega^2 \gg \alpha_0^2$ (this case: $\omega = 7.7 \times 10^5 s^{-1}$, $\alpha_0 = 2.8 \times 10^4$ s^{-1}) to

$$\eta = 1 - \alpha_0/\alpha_1 \quad (6)$$

In Fig. 2, values of α_1 are plotted as a function of U. Figure 3 shows values of E_{tot}, η, and E_{pl} as functions of U. It must be realized, however, that the accelerated plasma remains only a short time $t = t_2 - t_1$ in the influence of the coil

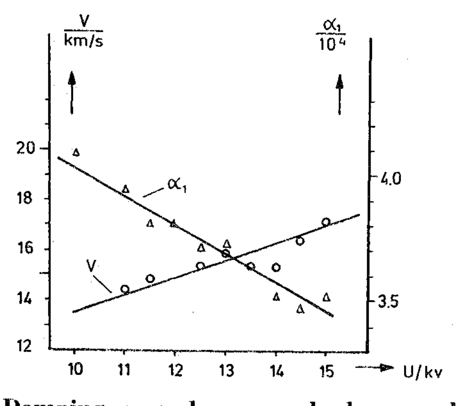

Fig. 2 Damping α_1 and measured plasma velocity vs capacitor voltage U.

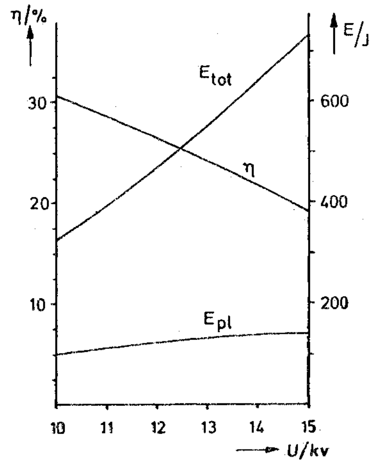

Fig. 3 Comparison of the total and absorbed energy as well as the efficiency.

and the effective efficiency is therefore

$$\eta_{eff} = E_{pl}/E_T = \eta\chi \quad (7)$$

where

$$E_T = \int_{t_1}^{t_2} R_1 I_1^2(t)dt$$

A corresponding calculation yielded χ = 3.

The plasma velocity is determined by measuring the onset of the light intensity pulses at three different positions along the acceleration tube. Results are given in Fig. 2.

The electron temperature T_e was determined from the ratio of the two He lines of subsequent ionization stages I_{II}/I_I:

$$I_{II}/I_I = C(1/b_{1,1}N_e)(kT_e)^{3/2}\exp(-52.5/kT_e) \quad (8)$$

where C contains atomic constants, $b_{1,1}$ is the ratio of the population density of the He II ground state to the corresponding Saha-Boltzmann density (tabulated in Ref. 4). The density N_e for T_e = 50,000°K was known from earlier measurements (see Ref. 5). A change of N_e with T_e could be estimated from the intensity of the He II (4686 Å) line. The ratio of the fourth level to the ground level of the He II ion, N_4/N_1 is calculated over a wide N_e and T_e range for a nonthermal plasma.[6] For these conditions N_1 is set equal to N_e with ± 30%;

$$N_4/N_1 \approx N_4/N_e = f(N_e, T_e) \quad (9)$$

Since $T_e(U)$ is known and I_{II} is proportional to N_4, then $N_e = N_e(U)$.

In Fig. 4, the temperature T_e is plotted as a function of U To calculate the thermal and kinetic energy of the plasma the total number of charged particles in the plasmoids must be known. The maximum density (≈1.2 × 10^{16}cm^{-3} for peak 1; ≈7.7 × 10^{15}cm^{-3} for peak 2) and the density distribution over the plasma length is nearly constant from 10 to 15 kv. The plasmoids have an annular shape and their volume was estimated in Ref. 5. Thus a total particle

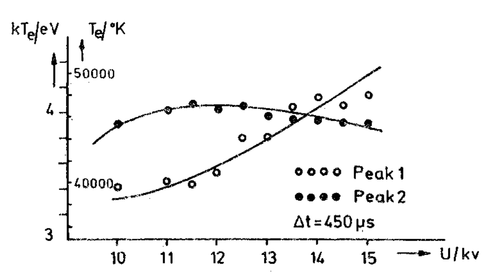

Fig. 4 Electron temperature of both plasmoids.

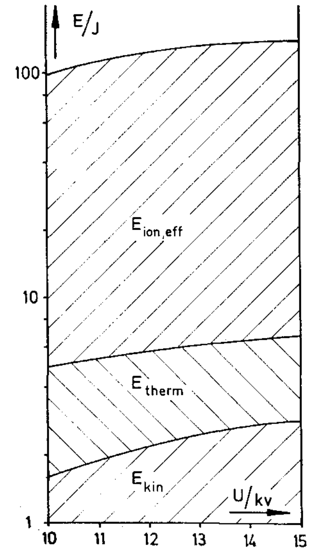

Fig. 5 Energy balance in function of capacitor voltage.

number of 2×10^{18} and 1×10^{18} for the 1st and 2nd plasmoid, respectively, is obtained.

In Fig. 5, the resulting energy balance is presented as a function of U. The effective ionization energy $E_{\text{ion,eff}}$ was calculated using Eq. (2).

Discussion

This investigation did not serve so much as to study the acceleration of a plasma, but rather to get information on a continuously working plasma source with a well-defined initial plasma velocity v. It can be seen from Fig. 2 that v varies slowly with U. As known from earlier investigations, the oscillating frequency f has a strong influence on v. This will be investigated by further measurements. Fig. 3 shows that an increase of E_{tot} up to a factor larger than two yields only an increase in E_{pl} of about 40%, because α_1 decreases with increasing U. The main portion of E_{pl} (Fig. 5) is needed for the ionization energy $E_{\text{ion,eff}}$ (more than 90%), whereas E_{kin} and E_{therm} attain only small values.

As seen from the energy balance (Fig. 5), $E_{\text{ion,eff}}$ per particle is about ten times the theoretical value which is 4×10^{-18} J/particle. Because of technical and physical reasons, the realizable range of particle flux $\dot{N}$ for continuously working accelerators is about $10^{20} - 10^{21}$ particles/sec. Thus, the necessary power requirement P_{pl} for such a source can be estimated approximately

$$P_{\text{pl}} \approx \dot{N}\ (\text{particles/s}) \cdot E_{\text{ion,eff}}(J/\text{particles})$$

Therefore, P_{pl} is 5 kw $\lesssim P_{\text{pl}} \lesssim$ 50 kw. The value of the effective efficiency of energy transfer η_{eff} (Eq. 7) was about 60–90% for the pulsed accelerator, so that assuming similar values for the continuous accelerator the power requirement must be divided by the corresponding η_{eff}.

References

[1] Wichmann, H. G., Meert, A., and Savary, M., "Über den Einfluss der Primärkreiskomponenten auf die Beschleunigung des Plasmas bei elektrodenlosen MHD-Triebwerken," *Jahrbuch der Wissenschaftlichen Gesellschaft für Luft- und Raumfahrt (WGLR)*, Vieweg-Verlag, Braunschweig, Germany, 1964, pp. 416–421.

[2] Meert, A., "Calculation of the Motion of an Idealized Plasma-Ring in Inductive Plasma Accelerators with Arbitrary Distribution of the Magnetic Field," *9th International Conference on Phenomena in Ionized Gases*, Editura Academiei Republicii Socialiste Romania, Bukarest, Rumania, Sept. 1969, p. 555.

[3] Meert, A., "Analysis of the Current Flow of a Condensor Discharge of an Electrodeless MHD-Motor," *Proceedings of the 30th Propulsion and Energetics Panel Meeting on New Experimental Techniques in Propulsion and Energetics Problems*, Advisory Group for Aerospace Research and Development (AGARD), Munich, Germany, Sept. 1967.

[4] Mewe, R., "Relative Intensity of Spectral Lines as a Function of Electron Temperature and Density," *British Journal of Applied Physics*, Vol. 18, 1967, pp. 107–118.

[5] Kohne, R., Meert, A., and Wichmann, H. G., "Theoretical and Experimental Investigations on Inductive Plasma Accelerators with Electromagnetic Standing Waves," *Proceedings of the 19th International Astronautical Congress*, Vol. 3, Propulsion and Re-entry Physics, Pergamon Press, PWN-Polish Scientific Publishers, New York, 1970, pp. 75–99.

[6] Drawin, H. W. and Emard, F., "Instantaneous Population Densities of the Excited Levels of Hydrogen Atoms, Hydrogen like Ions and Helium Atoms in Optically Thin Non-L.T.E. Plasmas," Rept. EUR-CEA-FC-534, Feb. 1970, Association Euratom-C.E.A., Fontenay-aux-Roses, France.

Laminated Orthotropic Plates under Transverse Loading

A. Holston Jr.*

Martin Marietta Corporation, Denver, Colo.

Introduction

THE use of high performance composites for lightly loaded structures leads to a small number of plies, thus producing asymmetrical laminates. These plates exhibit coupling between bending and stretching as was shown by Reissner and Stavsky[1] for two layer plates. Laminates which are symmetric about the reference surface do not produce coupling and behave as homogeneous anisotropic plates.

Stavsky[2] has established a linear theory for multilayer aeolotropic plates, based on the Kirchhoff hypothesis, and shown the reduction to a single eighth order equation for a generalized stress function. He gave solutions for cylindrical bending and uniform distribution of stress resultants and couples. Whitney and Leissa[3] have given a formulation for heterogeneous anisotropic plates and the reduction to three equations that are expressed in terms of displacements. They presented solutions for sinusoidal transverse loading, vibration, and buckling of cross-ply and angle-ply laminates. These plates have an even number of layers of the same thickness and elastic properties. The layers are alternately oriented at 0° and 90° to the plate axes for the cross-ply laminate and $\pm\theta$ for the angle-ply. Whitney[4] expanded each displacement in a double Fourier series and gave solutions for cross-ply and angle-ply plates under transverse load.

Whitney and Leissa[5] used a formulation in terms of a stress function and transverse displacement given by Dong, Pister and Taylor[6] and expanded both dependent variables in double Fourier series. They presented solutions for cross-ply and angle-ply plates under uniform transverse load, vibration and buckling. The Ritz technique was used by Ashton and Waddoups[7] to minimize the energy expression for symmetric anisotropic plates. Beam vibration modes were used for the assumed deflection functions and they studied displacement under lateral load, vibration and buckling.

This study uses the generalized stress function equation[2] and develops a Navier type of solution for simply supported, arbitrarily laminated, orthotropic plates under transverse loadings. The plate may have any number of orthotropic layers of arbitrary thicknesses and elastic properties with axes of elastic symmetry coincident with the plate axes. Deflection, stress resultants and couples are given explicitly

Received October 30, 1970.

* Senior Research Scientist. Member AIAA.